Geotechnical Aspects of Underground Construction in Soft Ground – Viggiani (ed)
© 2012 Taylor & Francis Group, London, ISBN 978-0-415-68367-8

The influence of jet-grout constitutive modelling in excavation analyses

M. Ciantia
Dipartimento di Ingegnieria Strutturale, Politecnico di Milano, Italy

M. Arroyo
Department of Geotechnical Engineering and Geosciences, UPC, Barcelona, Spain

R. Castellanza
Dipartimento di Ingegnieria Strutturale, Politecnico di Milano, Italy

A. Gens
Department of Geotechnical Engineering and Geosciences, UPC, Barcelona, Spain

ABSTRACT: A bonded elasto-plastic soil model is employed to characterize cement-treated clay in the finite element analysis of an excavation on soft clay supported with a soil-cement slab at the bottom. The soft clay is calibrated to represent the behaviour of Bangkok soft clay. A parametric study is run for a series of materials characterised by increasing cement content in the clay-cement mixture. The different mixtures are indirectly specified by means of their unconfined compressive strength. A similar parametric analysis is run in parallel using a linear elastic-perfectly plastic model for the clay-cement. Results from both series of analysis are compared highlighting the differences in predicted behaviour of the retaining wall and the excavation stability.

1 INTRODUCTION

Jet-grouted slabs are often employed in deep excavations in soft soils to reduce wall displacements and/or impermeabilize the excavation bottom (Eramo et al. 2011; Bitetti, 2007; Shirlaw, 2005). The slab has a structural role and its geometry and resistance need to be specified. While some simple design rules are available (JJGA, 2005; Shirlaw, 2005) a more in-depth analysis is sometimes necessary. A numerical simulation might be employed for the purpose, particularly if the movement of the retaining wall is required for design. The mechanical behaviour of the treated soil bodies is generally represented with simple models, typically the elastic perfectly plastic Mohr Coulomb model (e.g. Ho & Hu, 2006). One characteristic that is poorly represented by that type of models is brittleness of mechanical response, a basic trait of cemented geomaterials both natural and artificial.

On the other hand, brittleness is well captured by elasto-plastic bonded soil models (Gens & Nova, 1993). Bonded soil models have already shown their value with very diverse natural materials, from soft rocks like calcarenite (Lagioia & Nova, 1995) to very soft Holocene structured clays (Rouainia & Wood, 2000; Arroyo et al. 2008). Despite some early examples (Di Prisco et al., 1992), the application of bonded soil models to cement-improved soils has received somewhat less attention until very recently (Ciantia, 2009; Horpibulsuk et al., 2010).

One important obstacle to the practical application of bonded soil models is that they appear hard to calibrate. Nevertheless it is shown here that measuring porosity and unconfined compressive strength of the soil-cement and having knowledge of the amount of cement in the mixture is enough to initialize the main state variables of a bonded elasto-plastic model. Most of the other model parameters can be obtained from reconstituted samples of the treated soil.

A finite element model of a deep underwater excavation in clay partially sustained with a soil-cement slab is here employed as a trial case to study the influence in the excavation response of modelling the slab with a simple or a more refined constitutive model. The same measured properties of the slab are always assumed (unconfined compressive strength, porosity, cement content), but they are interpreted differently to initialize the different constitutive models being compared. We thus explore if the micro brittle response of the bonded model has consequences at the engineering scale.

2 BONDED SOIL MODEL

The bonded elasto-plastic model here employed is based on the CASM (Clay and Sand Model) developed by Yu (1998). The original CASM has been here both extended, (by introducing a new adimensional scalar history variable, *b,* representing "bonding") and modified (by using a different plastic potential formulation from that originally proposed).

The way the bonding variable enters the model follows closely the original proposal of Gens & Nova (1993). The yield surface is assumed to enlarge with increasing amount of bonding in the soil. Figure 1 shows the normal consolidation lines and yield surfaces for both unbonded and bonded materials with various amounts of bonding.

The yield surface can be expressed as follows:

$$f = \left(\frac{\sqrt{3}J}{M_\theta (p + p_t)} \right)^n + \frac{1}{\ln r} \ln \frac{(p + p_t)}{p_t + p_c} = 0 \qquad (1)$$

Where, as in the following, all the stresses are assumed effective. To obtain the behaviour shown in Figure 1,

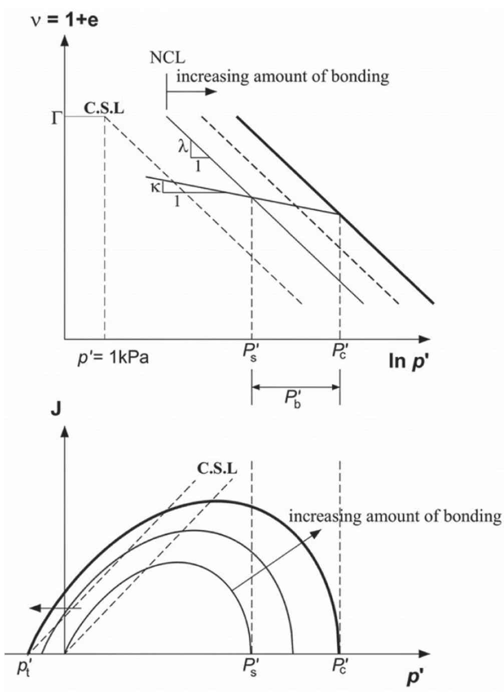

Figure 1. The normal consolidation lines (NCL), critical state lines (CSL) and yield surfaces for both unbonded and bonded materials.

$$\begin{aligned} p_c &= p_s (1 + b) \\ p_t &= p_s (\alpha_t b) \end{aligned} \qquad (2)$$

p_s is the preconsolidation pressure of the unbonded reference material. p_c controls the yielding of the bonded soil in isotropic compression and p_t the cohesion and tensile strength of the material; α_t is a parameter. The unbonded behaviour is recovered when *b* goes to zero.

In CASM the parameters *n* and *r* control the shape of the yield surface. M_θ is expressed as a function of Lode's angle θ, and determines the shape of the failure surface in the deviatoric plane, following a proposal by Sheng et al. (2000).

The plastic potential function has a similar form to the yield surface. One extra adjustment parameter, *m*, is introduced to allow the possibility of non-associated behaviour:

$$g = \left(\frac{m\sqrt{3}J}{M_\theta (p + p_t)} \right)^n + \frac{1}{\ln r} \ln \frac{(p + p_t)}{p_t + p_c} = 0 \qquad (3)$$

A classic volumetric hardening law is here employed for the unbonded material.

$$\frac{dp_s}{p_s} = \frac{d\varepsilon_v^p}{\lambda^* - \kappa^*} \qquad (4)$$

λ^* and κ^* are the compression parameters of the reconstituted clay, but referred to ε_v:ln *p* space.

Bonding (*b*) decreases exponentially with a plastic strain damage measure (*h*):

$$\begin{aligned} b &= b_0 e^{-h} \\ dh &= h_1 \left| d\varepsilon_v^p \right| + h_2 \left| d\varepsilon_s^p \right| \end{aligned} \qquad (5)$$

h_1 and h_2 are material parameters (greater than zero) defining the degradation rate. Further discussion of the CASM bonded model formulation and an example of its performance can be found at Gonzalez et al. (2009).

3 CALIBRATION PROCEDURE

3.1 *State variables*

Apart from the current stress state, the model includes two state variables: p_s and *b*. The calibration procedure for these state variables builds upon experimental work done on cement-mixed Bangkok clay by Bergado and co-authors (Lorenzo & Bergado, 2004; Horpibulsuk et al., 2004; Lorenzo & Bergado, 2006; Bergado et al, 2006). These authors work with controlled mixtures of reconstituted Bangkok clay and cement slurry, formed and cured in the laboratory.

Cement content on the mixture is specified by A_w, the ratio between cement weight and dry soil weight. It has been observed that the mechanical behaviour of the mixture is controlled by the ratio between current void ratio and cement content (e_{0t}/A_w). This mixing ratio accounts for the effects of initial clay water content, slurry water/cement ratio, slurry/clay mixing ratio and, because of using the current void ratio, curing time. Different combinations of these variables that result in the same mixture ratio (e_{0t}/A_w) show the same mechanical response.

Bergado and co-authors repeatedly proved the quantitative usefulness of that measure, obtaining good correlations with unconfined compressive strength, (Lorenzo & Bergado, 2004), oedometric yield points, (Horpibulsuk et al., 2004), peak resistance on undrained triaxial tests (Lorenzo & Bergado, 2006) and yield points on constant stress ratio drained triaxial tests (Bergado et al, 2006). For instance, in this latter case, they proposed the following empirical relation for the intersection of the yield surface of the mixture and the isotropic axis (units of measure kPa)

$$p_c = 0.49\left(\frac{e_{0t}}{A_w}\right)^2 - 31.9\left(\frac{e_{0t}}{A_w}\right) + 733 \tag{6}$$

In the relation above we have employed deliberately the symbol p_c to evidence the direct connection between this empirical relation and the model presented in the previous section. The particular formulation employed in (6) has some drawbacks and, to obtain a better fit to a wider range of experiments, can be advantageously substituted (Ciantia, 2009) by the following expression

$$p_c = F\left(\frac{e_{0t}}{A_w}\right) = k_1 e^{-k_2\left(\frac{e_{0t}}{A_w}\right)} + k_3 \tag{7}$$

where k_1, k_2 and k_3 are constants, taking the values 1188 [kPa], 0.046 [–] and 4 [kPa], respectively. Whatever the precise shape employed for the function F in (7) it follows from (2) that

$$b = \frac{F(e_{0t}/A_w)}{p_s} - 1 \tag{8}$$

On the other hand, p_s, the preconsolidation pressure of the unbonded reference material can be easily related to the current void ratio e_{0t} (Figure 1)

$$p_s = \exp\left(\frac{N - (1+e_{0t}) - \kappa \ln(p_{0t})}{\lambda - \kappa}\right) \tag{9}$$

Where p_{0t} is the current isotropic stress of the material (i.e. the stress concomitant with e_{0t}) and N is the ICL value at the reference pressure (p_a, here equal to 1 kPa).

Therefore, using equations (7) to (9) it is possible to initialize the model state variables (p_c, p_s) if the current void ratio and cement content of the mixture is known. Since the latter might not be always available, advantage might be taken of the good correlation that exists between unconfined compressive strength, q_u and mixture ratio. For instance, for cement-mixed Bangkok clay (Lorenzo & Bergado, 2004)

$$\left(\frac{q_u}{p_a}\right) = 10.33 e^{-0.046\left(\frac{e_{0t}}{A_w}\right)} \tag{10}$$

3.2 *Parameters of the reference material*

There are 8 parameters in the model that describe the mechanical response of the reference material (Table 1). Reconstituted Bangkok clay is assumed here as reference for the cement-treated Bangkok clay. While the geotechnical characteristics of the natural Bangkok clay have been object of much research (e.g. Balasubramaniam et al. 1978; Shibuya & Tamrakar 2003) the same does not apply to the reconstituted material. As many other soft clays, Bangkok clay is naturally endowed with a certain amount of structure and therefore its response is not always representative of that of the same material reconstituted. This made difficult the ideal approach to calibration of these parameters, which is by examining tests on the reference material only. Actually, it was only for the critical state friction angle (and hence for M) that such approach was possible (with data from Kamei et al. 2004).

Two alternative approaches were then employed. On the one hand, the classical Burland (1990) correlation between plasticity and reconstituted compressibility was used to obtain estimates of the relevant parameters (λ, N).

On the other hand, several aspects of the response of the reference material are predicted by the model to remain unaltered in the cement-mixed material. These aspects include the shape of the yield surface (controlled by parameters n and r), the degree of non-associativeness (controlled by parameter m) or the elastic response, (controlled by parameters κ and υ). Therefore such parameters can be also

Table 1. Parameters of the reference material.

N	λ	κ	M	n	r	m	ν
4	0.262	0.04	1.2	2	1.5	1.7	0.25

identified by observations on the improved material and that was the approach followed here. The resulting parameter set is collected in Table 1. More details about the calibration procedure are given by Ciantia (2009).

3.3 *Parameters of the cemented material*

The model parameters controlling behaviour of the cemented material are only three: the traction intercept parameter, α_t (eq. 2) and the degradation rate parameters, h_1 and h_2 (eq. 5). The value of α_t was estimated at 0.3 based on the yield surfaces reported by Bergado et al (2006). The value of the ratio h_1/h_2 was assumed equal to 3, following results for naturally cemented clay from Callisto & Rampello (2004).

The parameter controlling bond degradation rate, h_1, was obtained from simulations of oedometer tests for a single mixture (A_w = 10%). As already observed by Arroyo et al (2008) for Bothkennar clay, it appeared that the h_1 parameter that best suited the experiments was variable with the initial bonding of the material, b_0. The following dependency was then established

$$h_1 = 0.83\ln(b_0) + 1.77 \tag{11}$$

This result points to a shortcoming of the Gens & Nova bond evolution rule (5), which is unable to accommodate the high sensitivity of bond degradation rate to initial bonding. Alternative rules, with higher order dependency on initial bonding have been formulated, for instance, by Lagioia & Nova (1997).

3.4 *Illustrative results*

The model thus calibrated was verified against an extended database of oedometric tests and triaxial CIU tests on various mixtures of clay-cement (Ciantia, 2009). One example of the simulation results obtained is illustrated in Figure 2, where the stress-paths predicted for several undrained triaxial tests are displayed alongside the experimental results. It can be seen that the model has the potential to at least partly represent the "snap-back" traces that are typical of these softening materials. It is worth mentioning that, if the same tests are run using an elastic-perfectly plastic model such as the MC model, no such snap-back behaviour is observed and the stress path traces remain at their peak.

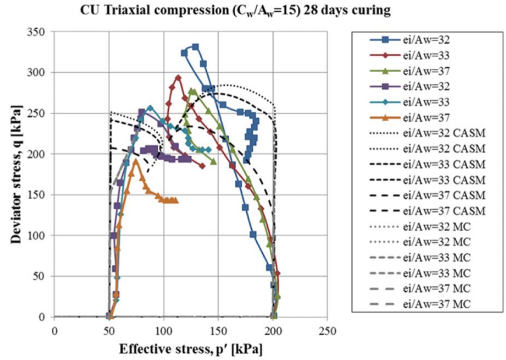

Figure 2. Simulation of undrained triaxial compression tests on cement-improved Bangkok clay. Experimental results from Lorenzo & Bergado (2006).

4 APPLICATION TO EXCAVATIONS

4.1 *Numerical implementation*

The bonded soil model described above was imple-mented in the finite element code PLAXIS Version 8, which has a facility to implement user-defined (UD) soil models.

4.2 *Description of the case*

In practice, jet grout slabs are not common in Bangkok, possibly because deep excavations penetrate below the clay level into stiffer layers (Phienwej, 2009). An artificial case (Figure 3) was then built into a finite element model with the specific purpose of exploring the sensitivity of the analysis to the material characterization of the treated soil.

The case built had three layers of clay with normally consolidated clay below excavation level, an overconsolidated layer on the surface (labelled 3 in the figure, OCR = 3) and an intermediate medium-consolidated layer (labelled 4 in the figure, OCR = 2). All these clay layers were modelled using the bonded CASM model presented in section 2, but with no bonding (i.e. initializing b = 0). The model parameters in all layers were those previously established for the reconstituted Bangkok clay (Table 1). The stress state was initialized with the Plaxis in-built K_0 procedure.

A thick (1 m) concrete (E = 30 MPa) retaining wall was supported at 0.5 m below its head by a rigid strut (400 kN/m/m) and at its bottom by a 3 m thick layer of cement treated clay. The excavation maximum depth was set at 11 m. The excavation process is simulated as a sequence of uniform excavation steps, of 1 m depth each. The strut is activated after the first excavation step. All the simulations assumed undrained behaviour of all the soil layers involved (including the clay-cement).

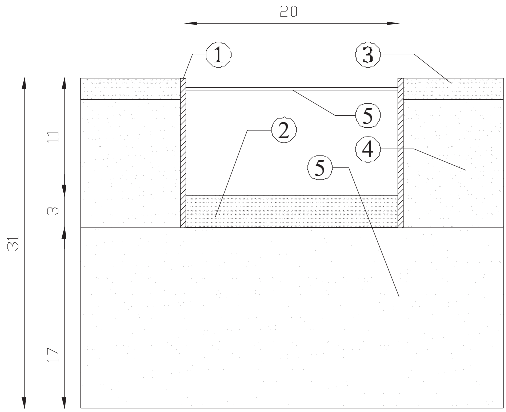

Figure 3. Schematic of the case analyzed.

4.3 *Parametric analysis*

A parametric analysis was performed employing two variables. The first was the constitutive model describing the behaviour of the clay-cement, which could be either a linear elastic-perfectly plastic model with Mohr-Coulomb yield (MC) or that described in the previous sections (bonded CASM). The other parameter was the unconfined compressive strength (UCS, q_u) of the clay-cement.

When the clay-cement was modeled using the MC model the only state variable of the material was stress. The initial stress of the slab was assumed isotropic and equal to the initial vertical stress. Four values of unconfined compressive strength were chosen for the parametric analysis (Table 2). Friction and dilatancy were neglected and strength was given by cohesion equal to half the UCS. Following common engineering practice for these materials, the Young's modulus was taken to be directly proportional to the UCS. The constant of proportionality assumed here was equal to 250, which is within the range found in the literature for jet-grout (e.g. Fang et al., 2006).

When the clay-cement mixture was modelled using the bonded CASM model a larger number of state variables required initialization. Clay-cement mixtures with the same UCS as in the previous case were the objective. To achieve that it was first necessary to make some assumptions about the initial clay water content (120% typical of Bangkok clay, Balasubramaniam et al., 1978), the water/cement (W/C) ratio in the slurry mixed with the clay (chosen as 1) and the curing time before the mixture attained the specified UCS (90 days, to allow for a fast but realistic construction schedule). Then, four values of cement content A_w were specified to attain the objective UCS. Note that the after curing void ratio value, e_{0t}, (which is the initial void ratio for the simulation) it is fixed once the previous mixture parameters have been specified. This was made following empirically-based expressions describing clay-cement mixture curing given by Lorenzo & Bergado (2006). Clearly, if a real case was to be simulated using this procedure, such an indirect evaluation of the soil-cement void ratio could be advantageously substituted by direct measurements on representative clay-cement field samples.

The main mixture properties corresponding to the different cases are collected in Table 3 below. Note that of all the mixture cement contents tabulated only the larger one (60%) is characteristic of jet-grouted mixtures, whereas the others are well below the typical range and more akin to those observed in deep soil mixing treatments.

Once the mixture properties are specified the state variables can be initialized using equations (6) to (8) above. The results obtained for the cases here analyzed are shown in Table 4.

Table 2. Variable parameters of MC model simulations.

Unconfined compressive strength q_u	Cohesion c	Young's modulus E
kPa	kPa	MPa
62	31	15.5
250	125	62.5
637	318	159
814	407	203

Table 3. Mixture properties for CASM model simulations.

Unconfined compressive strength q_u	Cement content by dry weight A_w	Initial void ratio e_{0t}	Mixture ratio e_{0t}/A_w
kPa	%	–	–
814	60	3.28	5.47
637	30	3.24	10.8
250	10	3.12	31.16
100	6	3.08	51.48

Table 4. Initial state variables of CASM model simulations.

Unconfined compressive strength q_u	b	p_s	p_c
kPa	–	kPa	kPa
814	6777	0.14	927
637	4386	0.17	727
250	991	0.29	287
100	211	0.34	116

4.4 *Simulation results*

Only a few simulation results will be presented here. In Figure 4 the movements in a point located at the contact between the soil-cement slab and the retaining wall are represented for the four cases computed using the MC model, against the excavation stage. As a reference the results obtained in a simulation where no slab of soil-cement is present are also included in the graph. Figure 5 represents the same results but now for the cases computed using the bonded CASM model.

A first distinction can be made between those cases where the simulation attained the end of the excavation and those where it did not achieve the final excavation stage because of a numerical lack of convergence that is indicative of failure. Failure happened only for two cases: that without soil improvement and that where the soil improvement was smaller (A_w = 5%; UCS = 62 kPa). It is interesting, however, to note that a stable support is attained even for a relatively low-strength mixture (A_w = 10%; UCS = 250 kPa).

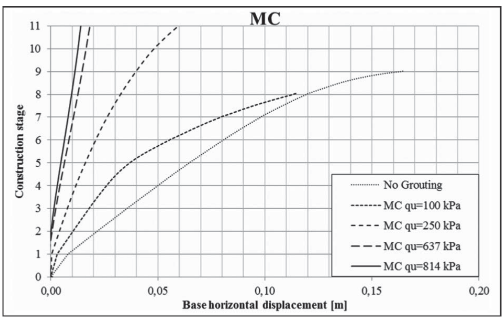

Figure 4. Horizontal displacement at the monitoring point vs excavation stage. Jet-grout slab modelled using MC.

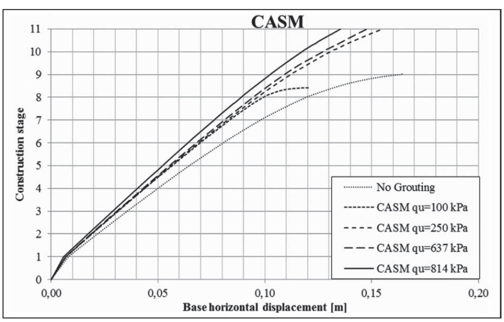

Figure 5. Horizontal displacement at the monitoring point vs excavation stage. Jet-grout slab modelled using CASM.

These results were true both for the simulations run using MC and for those run with the bonded CASM. Hence, from the point of view of predicting structure failure in absolute terms it was indifferent which constitutive model was employed. Note, however, that failure was attained for the cemented case (q_u = 62 kPa) at displacements much closer to the stable cases when using CASM than when using MC. This is an indication of structural brittleness, the kind of behaviour that would complicate the use of excavation monitoring as a preventive tool.

The choice of constitutive model for the clay-cement had also some important consequences for the stable cases. Displacements of the wall monitoring point were between 3 and 10 times higher when the improved soil slab was modeled using the bonded CASM than when it was modeled using the MC model.

It is also clear that the amount of displacement predicted by the bonded CASM was far less sensitive to the UCS of the mixture. Going from a q_u of 250 kPa to one of 814 kPa (or from a cement content of 5% to one of 60%) did only improve marginally the wall movement (Figure 5). When the clay-cement was modeled with the MC model, the stiffness of the structural response was clearly improved with increased UCS (Figure 4).

Similar observations can be made if the movement of the whole wall is considered. For the CASM model cases (Figure 6) the improved slab stiffness is always well below that of the head strut support, and an inverted cantilevered profile develops for all cases. For the MC model cases (Figure 7) there is a clear transition between low-motion and

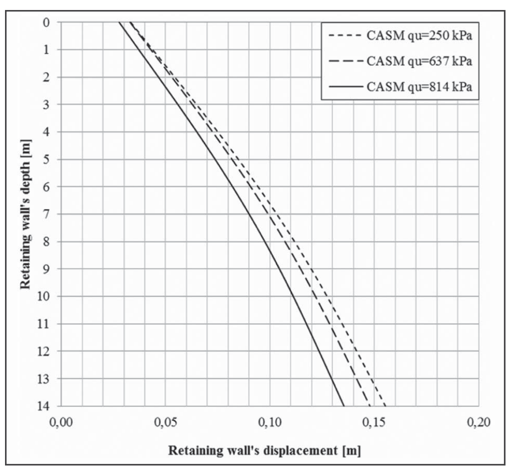

Figure 6. Horizontal displacement of the retaining wall vs depth. Jet-grout slab modelled using CASM.

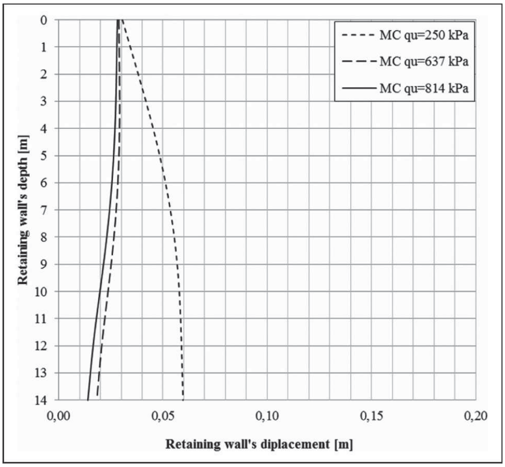

Figure 7. Horizontal displacement of the retaining wall vs depth. Jet-grout slab modelled using MC.

higher-motion cases in the strength range explored. It is clear that, for the higher strength cases, the wall movements predicted with the CASM model would have more serious implications in a real case, were the excavation is often surrounded by sensitive structures.

5 CONCLUSIONS

There are still some uncertain areas in the application of models such as the bonded CASM to real structures. The main one is that the laboratory behaviour that has been matched by the model corresponds to mixtures of relatively low-cement content cured at low pressures. It is unclear if the behaviour of field mixtures, cured under stress and, at least for most jet-grouted cases, generally containing higher cement contents than those explored here would be equally matched by the model.

However, from the results presented in this paper it can be already concluded that the use of an advanced constitutive model like the bonded CASM model will not be indifferent for the design of clay cement slabs supporting retaining walls. It appears that, for the same UCS, far larger movements might be predicted for the structure. Also, when failure appears, it happens in a more sudden manner. These results suggest that caution should be exercised if a simplified approach is used as a base for design.

Finally, it should be emphasized that the use of a model such as the bonded CASM would shifts the design emphasis from one based on the measurement of brittle material outcomes (like UCS) to one based on specified mixture properties (like cement content). Such an approach would clearly simplify control and field quality assessment procedures.

ACKNOWLEDGEMENTS

We are grateful to Nubia Gonzalez, from UPC, who provided the Plaxis subroutine coding the cemented CASM model and solved many numerical doubts. The support of the Spanish Ministry of Science through research grant BIA2008–06537 is also gratefully acknowledged.

REFERENCES

Arroyo, M., González, N., Butlanska, J., Gens, A. & Dalton, C. (2008) SBPM testing in Bothkennar clay: structure effects, *Geotechnical and Geophysical Site Characterization–Huang & Mayne (eds)* Taylor & Francis Group, London, 456–462.

Balasubramaniam, A.S., Hwang, Z.M., Uddin, W., Chaudhry, A.R. & Li, Y.G. (1978) Critical state parameters and peak stress envelopes for Bangkok clays, *Quarterly J. of Eng. Geol. and Hydrogeology*, 11, 219–232.

Bergado D.T., Taechakumthorn C., Lorenzo G.A. & Abuel-Naga H.M. (2006). Stress deformation behavior under anisotropic drained triaxial consolidation of cement treated soft Bankok clay, *Soils and Foundations*, Vol. 46, No. 5, 629–637.

Bitetti, B. (2007) Monitoraggio dei lavori di costruzione della linea B1 della metropolitana di Roma, *Incontro annuale dei Ricercatori di Geotecnica, IARG 2007,* Salerno, 4–6 Luglio 2007.

Burland, J.B. (1990) On the compressibility and shear strength of natural clays, Geotechnique 40:33, 329–378.

Callisto L. & Rampello, S. (2004) An interpretation of structural degradation for three natural clays. Can. Geotech. J. 41: 392–407.

Ciantia, M.O. (2009) *Modellazione del comportamento meccanico di terreni fini trattati con cemento*, Tesi di Laurea, Facolta di Ingegnieria, Politecnico di Milano.

Di Prisco C., Matiotti R., Nova R., (1992). A mathematical model of grouted sand allowing for strength degradation, *Numerical Models in Geomechanics*, 25–35.

Eramo, N., Modoni, G. & Arroyo, M (2011) Design, control and monitoring of a jet grouted excavation bottom plug, *7th International Symposium on Geotechnical Aspects of Underground Construction in Soft Ground.*

Fang, YS, Kao, CC, Chou, J, Chain, KF, Wang, DR & Lin, CT (2006) Jet grouting with the superjet-midi method, *Ground Improvement*, 10,2, 69–76.

Gens A., Nova R. (1993). Conceptual bases for a constitutive model for bonded soils and weak rocks, *Geotechnical Engineering of hard soils-soft rocks*, 485–494.

Gonzalez, N., Arroyo, M. & Gens, A. (2009) Identification of bonded clay parameters in SBPM tests: a numerical study, *Soils and Foundations* 49, 3, 329–340.

Ho, C.E. & Hu, S. (2006) Numerical analysis of jet grout elements for braced excavation in soft clay, ASCE Geocongress 2006 Geotechnical Engineering in the Information Technology Age, (doi 10.1061/40803(187)260).

Horpibulsuk, S., Liu, M.D., Liyaparathina, D.S. & Suebsuk, J. (2010) Behaviour of cemented clay simulated via the theoretical framework of the Structured Cam Clay model, Computers & Geotechnics, 37, 1–9.

Horpibulsuk S., Bergado D.T., Lorenzo G.A. (2004). Compressibility of cement-admixed clays at high water content, Geotechnique 53, No. 2, 151–154.

JJGA (Japan Jet Grout Association) (2005) Jet Grouting Technology (JSG method, Column Jet Grout method) Technical Information. 13th Edition (October 2005). Unofficial translation by T. Inui, K. Soga, H. Ji & Y. Ando.

Kamei, T., Tanaka, M. & Hayashi, S. (2004) Comparison of shear characteristics of undisturbed and remoulded Bangkok clay, Mem. Fac. Sci. Eng. Shimane Univ., 38, pp. 1–7.

Lagioia R. & Nova R., (1995) An experimental and theoretical study of the behaviour of a calcarenite in triaxial compression, *Géotechnique*, 45, 4, 633–648.

Lorenzo G.A., Bergado D.T. (2004). Fundamental parameters of cement-admixed clay—New approach, *Journal of geotechnical and geoenviromental engineering ASCE*, 1042–1050.

Lorenzo G.A., Bergado D.T. (2006). Fundamental characteristics of cement-admixed clay in deep mixing, Journal of materials in civil engineering, ASCE, 161–174.

Phienwej, N. (2009) Ground movements in station excavations of Bangkok first MRT, *Geotechnical Aspects of Underground Construction in Soft Ground-Ng, Huang & Liu (eds)* Taylor & Francis, 181–186.

Porbaha A., Raybaut J.L., Nicholson P. (2001). State of the art in construction aspects of deep mixing technology, Ground improvement, 3, 132–140.

Rouainia, M. & Wood, D.M. (2000) A kinematic hardening constitutive model for natural clays with loss of structure, *Géotechnique*, 50, 2, 153–164.

Sheng D, Sloan S.W. & Yu, H.S. (2000). Aspects of finite element implementation of critical state models. *Computational Mechanics* 26, 185–196.

Shirlaw, J.N. (2004) Jet grouting soft clays for tunnelling and deep excavations–design and construction issues, in Johnsen, Byle & Bruce (Eds), *Grouting and Ground Treatment: Proceedings of the Third International Conference*, February 10–12, 2003, New Orleans, Louisiana, ASCE.

Shibuya S., Tamrakar S.B. (2003). Engineering properties of Bangkok clay, Characterisation and Engineering Properties of Natural Soils—Tan et al. (Eds.) Sweets & Zeitlinger, Lisse, 645–692.

Yu, H.S. (1998). CASM: A unified state parameter model for clay and sand. *International Journal of Numerical and Analytical Methods in Geomechanics*, No. 22, 621–653.